IEEE Access
Multidisciplinary ⋮ Rapid Review ⋮ Open Access Journal

Received August 12, 2020, accepted October 23, 2020, date of publication November 16, 2020, date of current version November 30, 2020.

Digital Object Identifier 10.1109/ACCESS.2020.3037787

Outage and Throughput Analysis of Cognitive Users in Underlay Cognitive Radio Networks With Handover

SAMUEL D. OKEGBILE[1], **(Graduate Student Member, IEEE), BODHASWAR T. MAHARAJ**[1], **(Senior Member, IEEE), AND ATTAHIRU S. ALFA**[1,2], **(Member, IEEE)**

[1]Department of Electrical, Electronic and Computer Engineering, University of Pretoria, Pretoria 0002, South Africa
[2]Department of Electrical and Computer Engineering, University of Manitoba, Winnipeg, MB R3T 2N2, Canada

Corresponding author: Samuel D. Okegbile (samokegbile@gmail.com)

This work was supported by the SENTECH Chair in Broadband Wireless Multimedia Communications (BWMC), Department of Electrical, Electronics and Computer Engineering, University of Pretoria, South Africa.

ABSTRACT Interference characterization in cognitive networks with handover has received less attention in stochastic geometry-based interference management and control, especially in cognitive radio networks, because of the possibility of complicating the analysis of various performance metrics of interest, such as outage probability and throughput. However, because of the possible mobility that is observed in real practical systems, some of the receivers may be located outside the coverage regions of their paired transmitters. In order to ensure that any receiver located outside the coverage region of its paired transmitter continues to receive its required service from its paired transmitter while still achieving tractable analysis for various performance metrics of interest, we adopted multiuser diversity via packet relaying. With this approach, any secondary nodes waiting to transmit can be used to sustain coverage between any typical active transmitter and receiver pair, while reducing their own waiting period in the process. We obtained tractable analysis for outage probability, spectral efficiency and throughput and showed the effect of handover rate over the network performance. The outcomes of the numerical results show that the proposed approach is capable of improving the overall network performance by improving coverage and throughput among network users in the cognitive radio networks.

INDEX TERMS Handover cost, handover rate, multiuser diversity, outage probability, throughput.

I. INTRODUCTION

The continuous demand for an effective and efficient data transmission service has necessitated the exploration of the benefits of the cognitive radio network (CRN) in tackling the issue of spectrum scarcity. CRN provides an opportunity to accommodate more users on the network by allowing unlicensed users, called secondary users (SUs), to make use of channels assigned to licensed users, also known as primary users (PUs), through channel sensing. With more users now expected on the network, interference becomes an important factor, which if not properly managed can derail the essence of CRN. Hence, interference management and control have been receiving great attention in the last two decades.

The associate editor coordinating the review of this manuscript and approving it for publication was Wei Wang.

One useful approach to characterize interference in a wireless communications network is the adoption of stochastic geometry (SG), because of its ability to produce tractable analysis, especially when nodes are assumed to be independently and identically distributed following the Poisson point process (PPP) [1], [2]. Subsequent efforts have considered the introduction of exclusion regions around active PUs in which no SU is allowed to transmit. A similar concept is now being applied at secondary networks to enhance SUs' quality of service (QoS). With the introduction of exclusion regions in CRN, coverage in both primary and secondary networks can be improved at the expense of SUs' spectral usage efficiency, albeit under the assumption that all users are static. In order to capture the possible handover in the system modeling while still achieving an acceptable level of coverage and spectral efficiency for low-mobility users, multiuser diversity can be adopted in the domain of CRN.

Multiuser diversity not only allows efficient usage of spectral resources, but can also improve network performance through the creation of diverse independent transmission paths between any typical transmitter and receiver pair. Mobility can result in dynamic network topology over time, which may improve network throughput [3]. While the introduction of mobility is expected to improve overall network performance, its adoption in SG-driven interference management and control techniques has received less attention in CRN because of the possibility of complicating the analysis of various performance metrics of interest, such as outage probability and throughput. However, in practical systems, some users may be located outside the coverage regions of their paired transmitters owing to possible mobility. Investigating the impact of such a scenario on the network performance in CRN is hence very important. The coverage region is defined as the area within which the transmission signal power of any test transmitter is strong enough to ensure successful reception at its paired receiver. In this paper, this coverage region is the same as the protection region.

Users located outside the coverage region because of mobility can now take advantage of multiuser diversity to improve spectral usage efficiency. With mobility, several issues, such as spectrum handoff and channel selections, can complicate analysis [4], while characterizing interference in both primary and secondary networks is also more difficult, especially when the assumption of independence among users is relaxed. Various mobility issues in CR cellular networks were considered in [4], [5]. As a typical mobile user moves away from its source, there is a possibility that such a user traverses among diverse networks with different transmission frequencies, leading to frequent handoff – an occurrence that heavily deteriorates users' QoS [6]. Management of handover in dense cellular networks [7], [8] and dense 5G networks [9] was considered, using coverage probability and throughput to identify the effects of handover on the network, while the two-tier cellular network velocity aware handover management scheme considered in [10] is capable of sacrificing the best signal-to-noise plus interference ratio (SINR) association so as to reduce the handover rate and its effect. In these scenarios, SINR was derived based on stationary PPP analysis [7], [8], [10] to ensure tractability and was verified through simulations in order to demonstrate its accuracy, with the test user assumed to move at a constant velocity [8], [10]. It is worth noting that these efforts are based on the cellular network in which a typical mobile user is able to change its association whenever it moves away from the serving base station (BS) towards another BS. This idea allows the mobile user to initiate an association with a target BS if it is closer than the serving BS and terminate its existing association with the serving BS. Such a method means any typical mobile user can get its required service or connection from any active BS, an approach that is not suitable in a typical cognitive network considered in this work, where a tagged receiver can only get its required service through either direct or indirect association with its corresponding tagged transmitter. In such a case, a typical receiver cannot be disconnected from its paired transmitter.

Multiuser diversity has been demonstrated to be aided by packet relaying in wireless networks [3], [11]–[22]. In these works, the source and destination were demonstrated to be aided by a full duplex multiple input multiple output (MIMO) relaying node in [11], [22], time switching based half duplex relaying techniques [12], vertical cooperative relay [13], [16], [17], incremental relaying [21], cooperative relay [23], and full duplex based two-way amplify and forward relaying [24]. With the introduction of relaying techniques, several metrics of interest, such as success probability and ergodic capacity [11], outage probability [12], [13], [24], symbol error probability and channel capacity [24], can be used to evaluate the performance of the network. The relaying technique can be implemented as half duplex radios [12], [13], [18], full duplex radios [24], decode and forward nodes [12], [18], amplify and forward nodes [24], time switching relaying [16] etc, depending on the interests of the authors. Although full duplex relaying is expected to be more efficient than the half duplex technique, there is a possibility of self-interference in the former. The introduction of relaying techniques also enhances the idea of cooperative communication known as virtual MIMO techniques [24], which can improve network performance even when users are mobile. This cooperative communication can be in the form of horizontal cooperation or vertical cooperation [13]. In horizontal cooperation, PUs or SUs cooperate among one another to increase transmission efficiency and throughput, while vertical cooperation ensures cooperation between PUs and SUs so as to aid the transmission opportunity probability for SUs.

In this work, we modelled interference in underlay CRN with handover using the stochastic geometry approach, considering the case where primary and secondary receivers may be located outside the coverage region of their tagged transmitters owing to mobility. To the best of our knowledge, such an area has received less attention, especially when characterizing interference using SG in the domain of CRN. The closest efforts to our work are the work of [3], where multiuser diversity was considered in mobile ad hoc networks, [13], [14] where vertical cooperation in static CRN was considered and [11], where relay nodes aid source and destination communications in a static MIMO network. In [25], we characterized interference at the mobile receivers in CRN. The analysis, however, did not capture important mobility factors such as spectral efficiency, handover rate and handover cost.

For any communication link in a mobile network, the time-variant nature of the channel strength is an important characteristic. Such variation can be well accommodated through the use of diversity [3]. In this paper, we adopted multiuser diversity in order to keep a typical receiver with low mobility within the reach of its corresponding transmitter when such a receiver moves away from the coverage region of its transmitter. The main contributions of this paper are thus summarized as follows;

TABLE 1. Summary of the notations used.

Notation	Definition
D	Radius of the primary coverage/protection region
d	Radius of the secondary coverage/protection region
Φ_p, λ_p	Point process and intensity representing active PTs
r_p, r_s	Distance between any primary and secondary transmitter-receiver pair
Φ_s, λ_s	Point process and intensity representing all STs
Φ_s^m, λ_s^m	Point process and intensity representing active STs
Φ_r, λ_r	Point process and intensity of STs selected as relaying nodes at any time slot
P_p, P_s	Primary and secondary users' transmit powers
$V_{\min}, V_{\max}$	Minimum and maximum velocities
$\mathcal{L}_I$	Laplace transform of I

- We modelled the association between primary transmitters (PTs) and primary receivers (PRs) as well as secondary transmitters (STs) and secondary receivers (SRs), taking into consideration that PRs and SRs may be located within or outside the coverage area of their respective paired PTs and STs. Hence, when a tagged receiver is located within the coverage region of its corresponding transmitter, communication between the pair is achieved following the direct transmission method without the help of the relaying technique. However, when the tagged receiver is located outside the coverage region of its paired transmitter owing to mobility, communication between the transmitter-receiver pair is achieved through the packet relaying technique. In such a case, a tagged transmitter is considered to select any waiting secondary node that produces the highest signal at the tagged receiver through the multiuser diversity technique - a technique that can lead to handoffs. Multiuser diversity via packet relaying for mobile nodes was first proposed in [3].
- With the adoption of multiuser diversity, we obtained expressions for SINR for two cases: when multiuser diversity is adopted in a primary network (via vertical cooperation) for the purpose of reducing outage and when it is adopted in a secondary network (via horizontal cooperation) to improve spectral efficiency.
- Based on the SINR expressions derived for each of the cases considered, we carried out outage probability analysis in both primary and secondary networks. Our analysis takes into consideration the dependence between the distribution of PUs and SUs.
- Following the analysis of outage probability in both primary and secondary networks, we derived expressions for spectral efficiency and throughput while considering the effects of vertical handoff [26], [27] and horizontal handoff [26] through analysis of the handover rate and handover cost in both networks.

The remainder of this paper is structured as follows: In Section II, we present the details of the system model, while the analysis of SINR and outage probability are presented in Section III. In Section IV, an analysis of the network throughput is presented. Section V presents numerical results obtained through simulations, while Section VI concludes the paper and offers suggestions for future research. The summary of the notations used in this paper is given in Table 1.

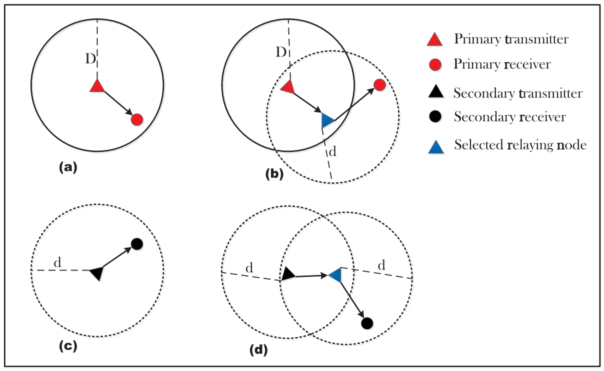

FIGURE 1. Representation for (a) direct association between PT and PR, (b) indirect association between PT and PR, (c) direct association between ST and SR, and (d) indirect association between ST and SR.

II. SYSTEM MODEL

In a typical CRN where SUs are allowed to make use of PUs' channels as long as their transmissions do not cause excessive interference at the primary network, some of the users are expected to be mobile when a practical system is considered. As a result of the mobility involved, there is constant change in the network topology, though the distribution of users is expected to remain unchanged. Since PU transmitters in CRN are normally radars, TV stations and cellular base stations licensed to use their respective assigned channels, we considered such devices to be located in a fixed location (or at least restricted to within their protection regions when mobile in order not to violate channel allocation policy), while any typical PR located outside the coverage of its paired PT is likely to experience loss of connection from its paired PT. Such a PR can take advantage of vertical cooperation to sustain its association or connection with its corresponding transmitter. However, STs make use of the spectrum in an opportunistic manner and a typical ST is not expected to move off its protection region, though communication can be sustained with the mobile SR located outside the coverage of its paired transmitter via horizontal cooperation.

Without loss of generality, we considered a transmitter-centric scenario as shown in Fig. 1, in which a typical PT is located at the center of a disk (known as the protection region) of radius D (see Fig. 1a and Fig. 1b) and a typical ST is located at the center of a disk of radius d (see Fig. 1c and Fig. 1d). It is worth noting that transmitters (either PTs or STs) are not necessarily located at the center of their respective protection zones, but this has been assumed for simplicity. This, however, is not a limitation on the distributions of users. We considered the protection zone of each transmitter to be the same as the coverage area of such transmitter [28], [29]. This implies that the signal generated by a typical transmitter is not strong enough outside its protection zone to satisfy the SINR requirement.

The introduction of a protection zone of radius D around each active PT means the distribution of active PTs can be best represented as the Matern hard core process. However, because its probability generating function is not available [2], [30], the distribution of active PTs was approximated as a PPP Φ_p of intensity λ_p, obtained through an approximation using equidense PPP, while each mobile PR y_i^p was initially considered to be located at a random distance r_p uniformly distributed as $f_{r_p}(l) = \frac{2l}{D^2}, \forall l \leq D$ around the location of its paired PT $x_i^p \in \Phi_p$.

On the other hand, STs are distributed according to independent PPP Φ_s of intensity λ_s and are not allowed to be active inside any PU's protection zone, or inside any currently transmitting ST's protection zone, in order to avoid interference at the primary network while improving SUs' QoS. Hence, the locations of active STs follow a modified version of the Poisson hole process Φ_s^m of intensity λ_s^m while each active mobile SR is similarly considered to be initially located at a random distance r_s following the uniform distribution given as $f_{r_s}(l) = \frac{2l}{d^2}, \forall l \leq d$ around the location of its corresponding transmitter.

When a typical ST $x_k^s \in \Phi_s$ is not eligible to transmit owing to its location, such an ST can serve as a decode and forward relaying node in either vertical or horizontal cooperation in order to improve channel efficiency while reducing its own waiting period in the process. As a tagged mobile receiver moves away from the coverage area of its pair tagged transmitter, the probability of outage increases. In order to sustain communication between the tagged transmitter and the tagged mobile receiver, the tagged transmitter through the multiuser diversity technique selects any waiting secondary node within its coverage region that generates the highest signal power[1] $w_{x_k^s}^{\max} = \max_{x_i^s \in \Phi_s} w_{x_i^s}$ at the paired receiver, where $w_{x_i^s}$ is the signal power generated by any ST $x_i^s \in \Phi_s$. The tagged transmitter hence sends its intended message to the selected relaying node(s) in the first hop. These selected nodes are known to be closer to the tagged receiver and provide higher capacity than the tagged transmitter under the Rayleigh fading of unit mean. During the second hop, each selected relay node (RN) sends the received packet to the intended receiver. Since the RNs are expected to be located closer to the tagged receiver (PR or SR) than the tagged transmitter (PT or ST) in this case, a better connection is achieved, provided that Rayleigh fading of unit mean is assumed. We further assumed that all RNs are capable of re-routing the received signal following the time switching based half-duplex technique, as in [12].

According to the random waypoint model [31], [32] in a discrete-time based system, each typical low mobility receiver uniformly selects its destination point D_k randomly within the deployment region, and moves to such destination by uniformly selecting a velocity v, $\forall v \in [V_{min}, V_{max}]$. At D_k, such a mobile receiver remains static for a predefined time t_p, before proceeding to the next destination following the same rule. Each receiver is considered to move independently, while updating its position at the beginning of each time slot. While the initial location of any tagged receiver can be assumed to follow a uniform distribution within the coverage region of its paired transmitter, the distribution of mobile receivers following a random waypoint model is non-uniform at the steady state [31]. The implication of non-uniformity of such a model is reduced in our proposed method, since the tagged receiver is not always located outside the coverage region of its paired tagged transmitter and can in fact be static during its transmission period.

The proposed approach can be summarized as follows:

- When a typical mobile PR is located at a distance $r_p \leq D$ from its paired PT, direct transmission is maintained between the primary transmitter-receiver pair. However, when such a tagged PR is located outside the coverage region of its paired PT, the SINR threshold requirement for coverage at the tagged PR may not be satisfied via direct transmission. Hence, the decode and forward ST nodes are used to sustain communication between the tagged PT and PR. The process is the same in the case of an ST and SR.
- To avoid interference resulting from multiple movements of packets from one node to another, the hop limit is restricted to two. A similar restriction was imposed in [33]. We further assumed that any selected relaying node would only be able to decode the destination address of the packet, but not the message itself, so as to ensure data security.[2] In such a case, a typical transmitter will transmit to the RN during the first hop, while each selected relay will transmit to the intended receiver during the second hop, provided there is at least one ST waiting to transmit within the coverage of such a typical transmitter and along the trajectory of the typical mobile receiver. We assumed that these RNs are capable of re-routing the received packet under vertical and horizontal cooperation by a distance of radius d.
- In a case where multiple potential RNs are located in the direction of a typical mobile receiver, the near

[1] We assumed that each inactive or waiting node generates a beacon at each time instant to indicate its presence in the channel.

[2] Although this is a simplistic assumption, there are many available known security schemes in the literature.

destination relay selection rule [13] through the multiuser diversity technique is followed.

- If there is no ST waiting to transmit within a tagged transmitter's coverage and along the trajectory of a tagged mobile receiver, the transmitter maintains direct association with the receiver. It is worth noting that higher ST intensity will produce higher spectrum opportunities, though with higher handoff rates.

This multiuser diversity based approach can be represented in terms of the presence of RN within the coverage region of any active transmitter as:

$$r_{x_j^s,D^*}[t] = \{0, 1\}, \quad \forall x_j^s \in \Phi_s, \ \forall t, \ \forall D^* = \{d, D\}, \quad (1)$$

where

$$r_{x_j^s,D^*}[t] = \begin{cases} 1 & \text{if there is RN within } D^* \text{ during time } t \\ 0 & \text{otherwise.} \end{cases}$$

By neglecting possible overlapping of protection regions in the primary network, a typical ST waiting to transmit within the coverage of a tagged PT cannot be located in the coverage region of another PT. Hence, any RN can serve at most one mobile PR at a time. Similarly, we assumed that a typical RN can only serve at most one mobile SR at a time. Hence,

$$\sum_{x_j^s \in \Phi_s} r_{x_j^s,D^*}[t] \leq 1, \quad \forall t, \ \forall D^*. \quad (2)$$

For primary transmission, the packet either moves from the tagged PT to the tagged PR under direct transmission or from any typical PT through the selected RNs to the paired PR following vertical cooperation. Similarly, for secondary transmission, the packet moves from any typical ST to its intended SR under direct transmission and from any typical ST to its intended SR via an RN following horizontal cooperation.

Although any tagged low mobility receiver (PR or SR) is expected to move with a velocity $v, \forall v \in [V_{min}, V_{max}]$, we considered $V_{min} \geq 0$ in order to capture the situations where such a receiver may be static, such that the probability density function of V [34] is given as

$$f_V(v) = \begin{cases} \frac{1}{V_{max}}, & \text{if } 0 \leq v \leq V_{max} \\ 0, & \text{otherwise.} \end{cases}$$

From this, the time in which any tagged low mobility PR resided in the coverage region of its paired PT and the time such PR spent in the coverage region of any selected RN can be known. Similarly, the time spent in the coverage region of its tagged ST and any selected RN by any tagged low mobility SR can be determined. From [34]–[36], we know that the expected mean time spent by the low mobility receiver in the coverage region of its tagged transmitter expressed as

$$E[T_{i_D^*}] = \frac{8D^* E[\frac{1}{V}]}{3\pi}, \quad (3)$$

and the expected mean time spent by such a receiver in the coverage region of the selected RN expressed as

$$E[T_{o_D^*}] = \frac{\pi d}{2E[V]}, \quad (4)$$

depend only on $E[\frac{1}{V}]$ and $E[V]$ respectively [36]. Next, we derive the analysis of outage probability in both primary and secondary networks.

Assumption 1: We assumed stationary point processes to model the distribution of users. Hence, the expressions for the outage probability are independent of velocity v.

Remark: Incorporating velocity v into the analysis of outage probability is very difficult and can complicate the analysis. Hence, the network topology was assumed to remain unchanged in each time slot and independent of the other time slots. The same assumption was made in [7], [8], [10] for cellular networks and was verified to be accurate through simulations.

III. ANALYSIS OF OUTAGE PROBABILITY

The outage probability is derived by determining the probability that the signal power received at a typical receiver is not above the predefined SINR threshold θ (i.e. $P(SINR \leq \theta)$). We derive the outage probability for PU and SU in the following subsections.

A. PRIMARY USER OUTAGE PROBABILITY

In order to derive an expression for the PT outage probability, two cases are considered - direct transmission between PT and PR and transmission from PT to PR via the selected relay nodes, depending on the required capacity, i.e. the number of packets n at any transmission time of PT. Generally, the PU outage probability can be given as

$$\mu_{out}^p = (1 - p_z)\varepsilon_p + p_z E(\varepsilon_{ind}), \quad (5)$$

where p_z is the probability that there is at least one ST waiting to transmit within the coverage area of the typical PT and along the trajectory of the typical mobile PR, ε_p is the PT outage probability under direct transmission and $E(\varepsilon_{ind})$ is the expected PT outage probability when a tagged PT transmits to its intending PR via RN(s). Although $p_z \in [0\ 1]$, its derivation can likewise be obtained from the Choquet capacity of a PPP [37] as $p_z = 1 - exp(-\lambda_s \pi D^2)$, where the definition of D is provided in [38] as

$$D = r_p \left[\theta_p \left(\frac{\zeta P_s}{P_p}\right)\right]^{1/\eta}, \quad (6)$$

where θ_p is the SINR threshold requirement for PUs' transmissions, ζ is a design factor [38] and η is the path loss exponent.

1) DIRECT TRANSMISSION BETWEEN PRIMARY TRANSMITTER-RECEIVER PAIR

Considering the case in which a typical PT located at point $x_k^p \in \Phi_p$ sends a direct message to its intended mobile PR located at point y_k^p within the coverage area of x_k^p, the SINR at the y_k^p can be expressed as

$$SINR_{y_k^p} = \frac{P_p c_{k,k} ||y_k^p||^{-\eta}}{\sigma^2 + I_{pp} + I_{sp} + I_{rp}}, \tag{7}$$

where $I_{pp} = \sum_{x_i^p \in \Phi_p \setminus x_k^p} P_p c_{i,k} ||y_i^p||^{-\eta}$ is the interference from other active PTs at the tagged PR, $I_{sp} = \sum_{x_i^s \in \Phi_s^m} P_s c_{i,k} ||y_i^p||^{-\eta}$ is the interference from active STs at the tagged PR and $I_{rp} = \sum_{x_i^s \in \Phi_s} P_r c_{i,k} ||y_i^p||^{-\eta}$ is the interference from active RNs at the tagged PR. P_p is the transmit power of PT, $c_{k,k}$ is the fading coefficient between the tagged transmitter and its intended receiver, $||y_k^p||$ is the Euclidean distance between the tagged PT and its intended PR, and σ^2 represents the Gaussian noise. Also, $c_{i,k}$ is the fading coefficient between other active transmitters and the tagged PR, $||y_i^p||$ is the Euclidean distance between other active transmitters and the tagged PR, P_s is the transmit power of ST and $P_r \approx P_s$ is the RN transmit power. We assumed that each channel multi-path fading is Rayleigh distributed with the unit mean (i.e $E[c] = 1$). The outage probability in this case is given in the following proposition.

Proposition 1: The outage probability at any tagged PR, given that the location of such a tagged PR is within the coverage area of its pair PT, can be expressed as

$$\begin{aligned}\varepsilon_p = 1 - \int_0^D & \exp\Big(-\frac{\theta_p}{P_p l^{-\eta}}\sigma^2\Big) \exp\Big\{-\pi \frac{\gamma \lambda_p (sP_p)^{\frac{\gamma}{\pi}}}{\sin(\gamma)}\Big\} \\ &\times \exp\Big\{-\pi \frac{\gamma \lambda_s (sP_s)^{\frac{\gamma}{\pi}}}{\sin(\gamma)}\Big\} \\ &\times \exp\Big\{-2\pi\lambda_p \int_D^\infty \Big(1-\exp(f(v))\Big) v dv\Big\} \\ &\times \exp\Big\{-\pi \frac{\gamma \lambda_r (sP_r)^{\frac{\gamma}{\pi}}}{\sin(\gamma)}\Big\} \\ &\times \exp\Big\{-2\pi\lambda_s^m \int_d^\infty \Big(1-\exp(f(w))\Big) w dw\Big\} \frac{2l}{D^2} dl,\end{aligned} \tag{8}$$

where $f(v) = \int_{v-D}^{v+D} cos^{-1}\Big(\frac{-D^2+v^2+r^2}{2vr}\Big) \frac{2\lambda_s r}{1+\frac{r^\eta}{sP_s}} dr$ and $f(w) = \int_{w-d}^{w+d} cos^{-1}\Big(\frac{-d^2+w^2+r^2}{2wr}\Big) \frac{2\lambda_s r}{1+\frac{r^\eta}{sP_s}} dr$. The intensity $\lambda_s^m = \lambda_s \rho_p \rho_s$, where $\rho_p = \exp(-\lambda_p \pi D^2)$ represents the probability that an active typical ST is not within the exclusion region of another active PT and $\rho_s = \exp(-\lambda_s \pi d^2)$ represents the probability that a typical ST is not within the exclusion region of another active ST. $\gamma = \frac{2\pi}{\eta}$, $\lambda_r \in \lambda_s$ is the intensity of inactive STs available as RN (knowing that the available RNs are a fraction of STs) and $s = \frac{\theta_p}{P_p l^{-\eta}}$.

Proof: Although the analysis of the outage probability is based on the use of stationary point process analysis, simulation results show that such analysis accurately captures the performance of mobile users. A similar conclusion was reached in [7], [10]. The derivation presented in Proposition 1 is straightforward from (7). The proof is summarized in Appendix A for brevity.

At $\eta = 4$, the ε_p can be simplified to

$$\varepsilon_p = 1 - \exp\Big(\frac{-\theta_p \sigma^2}{P_p r_p^{-4}} - \frac{\pi^2}{2}\lambda_p \sqrt{\theta_p} r_p^2 - \frac{\pi^2}{2}\sqrt{\frac{\theta_p P_s}{P_p}} r_p^2 (\lambda_s + \lambda_r)\Big). \tag{9}$$

2) INDIRECT TRANSMISSION BETWEEN PRIMARY TRANSMITTER-RECEIVER PAIR VIA VERTICAL COOPERATION

As a result of its ability to be mobile, a tagged PR may be located outside the coverage region of its paired PT. In such a case, the PT transmits to the PR through a relaying node or set of relays using a message splitting technique [15]. When message splitting is used, the PT message is divided into segments in order to meet the selected relay's capacity requirements. Any typical transmitter is able to generate the distance through signal strength from its paired receiver similar to the reference signal received power and reference signal received quality techniques in 4G long-term evolution.

Assumption 2: We assumed that the PT's message is divided into n number of segments depending on the n number of packets required to be transmitted. If packets do not arrive sequentially at the intending receiver, they simply wait to be re-assembled.

When the primary transmitter and receiver pair communicate via RN(s), outage is possible in two conditions. The first is the case in which the message is lost during the first hop (i.e. $SINR_{R_k}^I \leq \theta_p$) at any selected RN. This means that any of the selected RN(s) cannot decode the message from the PT, hence the message is lost during the first hop, i.e. $\prod_{n=1}^N SINR_{R_k}^I \leq \theta_p$, where $n = 1..N$ is the number of selected RNs. This implies that the intended PR cannot receive the PT message during the second hop. In such a case, the SINR received at the intended PR located outside the coverage of its paired PT in each hop is $SINR_{y_k^p}^I \ll \theta_p$. The other case is when the message is lost during the second hop, (i.e. $SINR_{y_k^p}^{II} \leq \theta_p$), which means all the selected RN(s) can decode the PT message (i.e. $\prod_{n=1}^N SINR_{R_k}^I > \theta_p$); however, the intended PR cannot decode the received PT message during the second hop. For simplicity and following Assumption 2, we assumed that each typical PT selects only one RN (i.e. has only one packet to send at any time, $n = 1$). The joint outage probability can then be obtained following the information theory formula [13], [21] as $P(I_c \leq R)$, where $\theta_p = 2^R - 1$, R being the rate at which the information is being sent [13] and I_c being given as

$$I_c = \begin{cases} \frac{1}{2}\log_2(1 + 2SINR_{y_k^p}^I) & SINR_{R_k}^I \leq \theta_p \\ \frac{1}{2}\log_2(1 + SINR_{y_k^p}^I + SINR_{y_k^p}^{II}) & SINR_{R_k}^I > \theta_p. \end{cases} \tag{10}$$

From (10), the expected outage probability under indirect transmission between any primary transmitter-receiver pair via SU relay ε_{ind} is obtained as

$$\varepsilon_{ind} = P(SINR^I_{R_k} \leq \theta_p)P(2SINR^I_{y^p_k} \leq \theta_p) + P(SINR^I_{R_k} > \theta_p)P(SINR^I_{y^p_k} + SINR^{II}_{y^p_k} \leq \theta_p). \quad (11)$$

The assumption of no correlation between the two hops as in [13] means (11) can be solved by deriving the outage probability expression for each of the segments involved. Hence, the SINR at any selected relay during the first hop is given as

$$SINR^I_{R_k} = \frac{P_p c_{k,k}||y^R_k||^{-\eta}}{\sigma^2 + I_{pr} + I_{RN} + I_{rr}}, \quad (12)$$

where $||y^R_k||$ is the Euclidean distance between the tagged PT and the selected RN, I_{pr}, I_{RN} and I_{rr} are the interference from other active PTs, interference from active STs and interference from active RNs at any typical selected RN (R_k) respectively. Note that the location of the RN is actually within the coverage area of the tagged PT. This implies that the SINR at R_k is the same as $SINR_{y^p_k}$ presented in (7). Hence, $P(SINR^I_{R_k} \leq \theta_p) = \varepsilon_p$.

The next step is to derive the outage probability analysis for $P(2SINR^I_{y^p_k} \leq \theta_p) = \varepsilon_1$.

$$\varepsilon_1 = P\left\{\frac{2P_p c_{k,k}||y^p_k||^{-\eta}}{\sigma^2 + I_{pp} + I_{sp} + I_{rp}} \leq \theta_p\right\}, \quad (13)$$

By Rayleigh fading assumption, (13) can be expressed as

$$\varepsilon_1 = 1 - \int_D^{D_1} \exp\left(\frac{-\sigma^2\theta_p}{2P_p l^{-\eta}}\right)\mathcal{L}_{I_{pp}}(s)\mathcal{L}_{I_{sp}}(s)\mathcal{L}_{I_{rp}}(s)\frac{2l}{D_1^2}dl, \quad (14)$$

where $D_1 = D + d$. The derivations of $\mathcal{L}_{I_{pp}}$, $\mathcal{L}_{I_{sp}}$ and $\mathcal{L}_{I_{rp}}$ are similar to the ones in Proposition 1 except that the Laplace transforms (LTs) were taken at $s = \frac{\theta_p}{2P_p l^{-\eta}}$.

The last part of (11) is $P(SINR^I_{y^p_k} + SINR^{II}_{y^p_k} \leq \theta_p) = \varepsilon_2$. Let the distance between the tagged PT and the selected RN during the first hop be r_{p2} and the distance between the selected RN and the tagged PR during the second hop be r_R in any typical two consecutive time slots; ε_2 is given as

$$\varepsilon_2 = E\{P(P_p c_{k,k} r_{p2}^{-\eta} + P_r c_{k,k} r_R^{-\eta} \leq \theta_p(\sigma^2 + I_{pp} + I_{sp} + I_{rp})\}, \quad (15)$$

$$\varepsilon_2 \overset{(a)}{=} 1 - \left(\frac{P_p r_R^\eta}{P_p r_R^\eta - P_r r_{p2}^\eta}\right)\{\exp(-s_1\sigma^2)\mathcal{L}_{I_{pp}}(s_1)\mathcal{L}_{I_{sp}}(s_1) \times \mathcal{L}_{I_{rp}}(s_1)\} - \left(\frac{P_r r_{p2}^\eta}{P_r r_{p2}^\eta - P_p r_R^\eta}\right)\{\exp(-s_2\sigma^2)\mathcal{L}_{I_{pp}}(s_2) \times \mathcal{L}_{I_{sp}}(s_2)\mathcal{L}_{I_{rp}}(s_2)\}, \quad (16)$$

where $s_1 = \frac{\theta_p}{P_p r_{p2}^{-\eta}}$ and $s_2 = \frac{\theta_p}{P_r r_R^{-\eta}}$. (a) is derived by obtaining the cdf of $P_p c_{k,k} r_{p2}^{-\eta} + P_r c_{k,k} r_R^{-\eta}$ in (15), which is given as $P(P_p c_{k,k} r_{p2}^{-\eta} + P_r c_{k,k} r_R^{-\eta} \leq \varkappa)$, where $\varkappa = \theta_p(\sigma^2 + I_{pp} + I_{sp} + I_{rp})$. By substituting (8), (14) and (16) into (11), (5) can be obtained.

B. SECONDARY USER OUTAGE PROBABILITY

The same process as in the analysis of PT outage probability was followed to derive ST outage probability under direct and indirect associations. For direct association, a typical ST transmits directly to its paired SR, while the transmission from ST to SR is directed via RN during indirect association. SU outage probability is thus given as

$$\mu^s_{out} = (1 - p_f)\varepsilon_s + p_f E(\varepsilon_{relay}), \quad (17)$$

where p_f is the probability that there is at least one ST waiting to transmit within the protection region of the typical ST and along the trajectory of the typical mobile SR, ε_s is the outage probability under direct transmission between the secondary transmitter-receiver pair and $E(\varepsilon_{relay})$ is the expected outage probability when a tagged ST transmits to its intended SR via the selected RN.

1) DIRECT TRANSMISSION BETWEEN SECONDARY TRANSMITTER-RECEIVER PAIR

In this case, a typical ST $x^s_k \in \Phi^m_s$ sends a direct message to its intended SR y^s_k considered to be located within its paired ST coverage area, otherwise known as the protection region of radius d. The SINR at the SR can be expressed as

$$SINR_{y^s_k} = \frac{P_s c_{k,k}||y^s_k||^{-\eta}}{\sigma^2 + I_{ss} + I_{ps} + I_{rs}}, \quad (18)$$

where $I_{ss} = \sum_{x^s_i \in \Phi^m_s \setminus x^s_k} P_s c_{i,k}||y^s_i||^{-\eta}$ is the interference from other active STs at the tagged SR, $I_{ps} = \sum_{x^p_i \in \Phi_p} P_p c_{i,k}||y^s_i||^{-\eta}$ is the interference from active PTs at the tagged SR and $I_{rs} = \sum_{x^s_i \in \Phi_s} P_r c_{i,k}||y^s_i||^{-\eta}$ is the interference from active RNs at the tagged SR. $||y^s_k||$ is the Euclidean distance between the tagged ST and its intended SR and $||y^s_i||$ is the Euclidean distance between any transmitter and the tagged SR. The outage probability in this case is given in Proposition 2.

Proposition 2: The outage probability at any tagged SR, given that the location of such a tagged SR is within the coverage area of its pair ST, can be expressed as

$$\varepsilon_s = 1 - \int_0^d \exp\left(-\frac{\theta_s}{P_s l^{-\eta}}\sigma^2\right)\exp\left\{-\pi\frac{\gamma\lambda_r(zP_r)^{\frac{\gamma}{\pi}}}{\sin(\gamma)}\right\} \times \exp\left\{-2\pi\lambda_s\rho_p\int_d^\infty \frac{r}{1 + \frac{r^\eta}{zP_s}}dr\right\} \times \exp\left\{-\pi\frac{\gamma\lambda_p(zP_p)^{\frac{\gamma}{\pi}}}{\sin(\gamma)}\right\} \times \exp\left\{2\lambda_p\int_{v-d}^{v+d} cos^{-1}\left(\frac{-d^2+v^2+r^2}{2vr}\right)\frac{r}{1+\frac{r^\eta}{zP_p}}dr\right\} \times \frac{2l}{d^2}dl, \quad (19)$$

where θ_s is the SINR threshold for SU and $z = \frac{\theta_s}{P_s r_s^{-\eta}}$.

Proof: The proof is presented in Appendix B.

At $\eta = 4$, the close form of (19) can be obtained as

$$\varepsilon_s = 1 - \exp\Big(\frac{-\theta_s\sigma^2}{P_s r_s^{-4}} - \lambda_s\rho_p\Big(\frac{\pi^2}{2}r_s^2\sqrt{\theta_s} - \pi\frac{\tan^{-1}(\frac{d^2}{\sqrt{\theta_s}r_s^2})}{\frac{1}{\sqrt{\theta_s}r_s^2}}\Big) - \frac{\pi^2}{2}r_s^2\Big(\lambda_p\sqrt{\frac{\theta_s P_p}{P_s}} + \lambda_r\sqrt{\theta_s}\Big)\Big). \quad (20)$$

2) INDIRECT TRANSMISSION VIA HORIZONTAL COOPERATION

A tagged SR may be located outside the coverage region of its paired ST owing to mobility. In such a case, the ST transmits to the SR through any selected RN, hence outage is possible under two scenarios: if outage occurs during the first hop (i.e. $SINR_{R_k} \leq \theta_s$) and if outage occurs during the second hop (i.e. $SINR_{R_k} > \theta_s$). The joint outage probability can then be similarly obtained following the information theory formula given as

$$I_{c2} = \begin{cases} \frac{1}{2}\log_2(1 + 2SINR^I_{y_k^s}) & SINR^I_{R_k} \leq \theta_s \\ \frac{1}{2}\log_2(1 + SINR^I_{y_k^s} + SINR^{II}_{y_k^s}) & SINR^I_{R_k} > \theta_s. \end{cases} \quad (21)$$

The outage probability ε_{relay} is thus given as

$$\varepsilon_{relay} = P(SINR^I_{R_k} \leq \theta_s)P(2SINR^I_{y_k^s} \leq \theta_s) + P(SINR^I_{R_k} > \theta_s)P(SINR^I_{y_k^s} + SINR^{II}_{y_k^s} \leq \theta_s). \quad (22)$$

From (22), we can obtain the SINR at any selected RN during the first hop as

$$SINR^I_{R_k} = \frac{P_s c_{k,k}||y_k^R||^{-\eta}}{\sigma^2 + I_{RN} + I_{pr} + I_{rr}}, \quad (23)$$

where $||y_k^R||$ represents the Euclidean distance between the tagged ST and the selected RN, while $I_{RN} = \sum_{x_i^s \in \Phi_s^m \setminus x_k^s} P_s c_{i,k}||y_i^R||^{-\eta}$, $I_{pr} = \sum_{x_i^p \in \Phi_p} P_p c_{i,k}||y_i^R||^{-\eta}$ and $I_{rr} = \sum_{x_i^s \in \Phi_s} P_r c_{i,k}||y_i^R||^{-\eta}$ are the interference from other active STs, interference from active PTs and interference from other active RN at the selected RN R_k respectively. Similarly, the location of the RN is actually within the exclusion region of the tagged ST, hence the SINR at R_k is the same as the one presented in (18). Hence, $P(SINR^I_{R_k} \leq \theta_s) = \varepsilon_s$.

Next, we derive the analysis for $P(2SINR^I_{y_k^s} \leq \theta_s) = \varepsilon_3$.

$$\varepsilon_3 = P\Big\{\frac{2P_s c_{k,k}||y_k^s||^{-\eta}}{\sigma^2 + I_{ss} + I_{ps} + I_{rs}} \leq \theta_s\Big\}. \quad (24)$$

$$\varepsilon_3 = 1 - \int_d^{2d} \exp\Big(\frac{-\sigma^2\theta_s}{2P_s l^{-\eta}}\Big)\mathcal{L}_{I_{ss}}(z)\mathcal{L}_{I_{ps}}(z)\mathcal{L}_{I_{rs}}(z)\frac{2l}{(2d)^2}dl. \quad (25)$$

Likewise, the derivations of $\mathcal{L}_{I_{ss}}$, $\mathcal{L}_{I_{ps}}$ and $\mathcal{L}_{I_{rs}}$ are similar to the ones in Proposition 2 except that each LT was taken at $z = \frac{\theta_s}{2P_s l^{-\eta}}$.

To obtain analysis for $P(SINR^I_{y_k^s} + SINR^{II}_{y_k^s} \leq \theta_s) = \varepsilon_4$, let the distance between the tagged ST and the selected RN during the first hop be r_{s2} and the distance between the selected RN and the tagged PR during the second hop be r_R in any typical two consecutive time slots; ε_4 is given as

$$\varepsilon_4 = E\{P(P_s c_{k,k} r_{s2}^{-\eta} + P_r c_{k,k} r_R^{-\eta} \leq \theta_s(\sigma^2 + I_{ss} + I_{ps} + I_{rs})\}, \quad (26)$$

$$\varepsilon_4 \overset{(a)}{=} 1 - \Big(\frac{P_s r_R^\eta}{P_s r_R^\eta - P_r r_{s2}^\eta}\Big)\{\exp(-z_1\sigma^2)\mathcal{L}_{I_{ss}}(z_1)\mathcal{L}_{I_{ps}}(z_1) \times \mathcal{L}_{I_{rs}}(z_1)\} - \Big(\frac{P_r r_{s2}^\eta}{P_r r_{s2}^\eta - P_s r_R^\eta}\Big)\{\exp(-z_2\sigma^2) \times \mathcal{L}_{I_{ss}}(z_2)\mathcal{L}_{I_{ps}}(z_2)\mathcal{L}_{I_{rs}}(z_2)\}, \quad (27)$$

where $z_1 = \frac{\theta_s}{P_s r_{s2}^{-\eta}}$ and $z_2 = \frac{\theta_s}{P_r r_R^{-\eta}}$. (a) is derived by obtaining the cdf of $P_s c_{k,k} r_{s2}^{-\eta} + P_r c_{k,k} r_R^{-\eta}$ in (26), which is given as $P(P_s c_{k,k} r_{s2}^{-\eta} + P_r c_{k,k} r_R^{-\eta} \leq \varkappa_s)$, where $\varkappa_s = \theta_s(\sigma^2 + I_{ss} + I_{ps} + I_{rs})$.

IV. ANALYSIS OF THROUGHPUT

Following the analysis of outage probability presented in the previous section, we obtained the analysis of average throughput in this section. According to [7], the average throughput is given as

$$AT = BS_E(1 - D_H), \quad (28)$$

where B, S_E and D_H are the overall bandwidth of the channel, average spectral efficiency, and handover cost (defined as the fraction of time in which no data are transmitted to the tagged receiver owing to the handover process) respectively. Note that handover occurs when a typical transmitter initiates a connection with any selected RN in order to sustain communication with its paired receiver. The average spectral efficiency is given as [2]

$$S_E = \int_0^\infty P\{\ln(1 + SINR) > z\}dz \overset{(a)}{=} \int_0^\infty \frac{P\{SINR > x\}}{x+1}dx \quad (29)$$

where (a) is obtained by making variables $x = e^z - 1$. At the primary network, the average spectral efficiency can be expressed as

$$S_E^p = \int_0^\infty \frac{1 - ((1 - p_z)\varepsilon_p + p_z E(\varepsilon_{ind}))}{x+1}dx. \quad (30)$$

Similarly, the average spectral efficiency at the secondary network is given as

$$S_E^s = \int_0^\infty \frac{1 - ((1 - p_f)\varepsilon_s + p_f E(\varepsilon_{relay}))}{x+1}dx. \quad (31)$$

As a typical mobile receiver moves along its trajectory, any selected RN may be used to sustain its association with its typical transmitter. This results in vertical handoff (when used in the primary network) and horizontal handoff (when used in the secondary network). It is worth noting that the proposed approach only makes use of ST as relaying nodes. Hence, D_H is simplified as given in [16] as

$$D_H = \min(H_o * d_e, 1), \tag{32}$$

where H_o is the handover rate and d_e is the handover delay. At constant velocity v with no pause time assumptions, H_o [39] is given as

$$H_o = \frac{4v}{\pi}\sqrt{\lambda_s}. \tag{33}$$

The average throughput in the primary network can be obtained by substituting (30) into (28), hence,

$$AT_p = B(1-D_H)\int_0^\infty \frac{1-((1-p_z)\varepsilon_p + p_z E(\varepsilon_{ind}))}{x+1}dx. \tag{34}$$

At $\eta = 4$, the average throughput in the primary network can be expressed as

$$\begin{aligned} AT_p &= B(1-D_H)\int_0^\infty 1-\Bigg((1-p_z)\Big\{1-\exp\Big(\frac{-\sigma^2 x}{P_p r_p^{-4}}-\frac{\pi^2}{2}\lambda_p \\ &\times\sqrt{x}r_p^2-\frac{\pi^2}{2}\sqrt{\frac{xP_s}{P_p}}r_p^2(\lambda_s+\lambda_r)\Big)\Big\}+p_z\Big\{\Big(1-\exp\Big(\frac{-\sigma^2 x}{P_p r_p^{-4}} \\ &-\frac{\pi^2}{2}\lambda_p\sqrt{x}r_p^2-\frac{\pi^2}{2}\sqrt{\frac{xP_s}{P_p}}r_p^2(\lambda_s+\lambda_r)\Big)\Big) \\ &\times\Big(1-\exp\Big(\frac{-\sigma^2 x}{2P_p r_{p2}^{-4}}-\frac{\pi^2}{2}\lambda_p\sqrt{\frac{x}{2}}r_{p2}^2 \\ &-\frac{\pi^2}{2}\sqrt{\frac{xP_s}{2P_p}}r_{p2}^2(\lambda_s+\lambda_r)\Big)\Big)+\Big(\exp\Big(\frac{-\sigma^2 x}{P_p r_p^{-4}} \\ &-\frac{\pi^2}{2}\lambda_p\sqrt{x}r_p^2-\frac{\pi^2}{2}\sqrt{\frac{xP_s}{P_p}}r_p^2(\lambda_s+\lambda_r)\Big)\Big)\times\Big(1-\exp \\ &\times\Big(\frac{-\sigma^2 x}{P_p r_p^{-4}+P_r r_R^{-4}}-\frac{\pi^2}{2}\lambda_p\sqrt{\frac{xP_p}{P_p r_p^{-4}+P_r r_R^{-4}}}-\frac{\pi^2}{2} \\ &\times\sqrt{\frac{xP_s}{P_p r_p^{-4}+P_r r_R^{-4}}}(\lambda_s+\lambda_r)\Big)\Big)\Big\}\Bigg)\frac{1}{x+1}dx. \end{aligned} \tag{35}$$

Similarly, the average throughput in the secondary network can be obtained by substituting (31) into (28). This is expressed as

$$AT_s = B(1-D_H)\int_0^\infty \frac{1-((1-p_f)\varepsilon_s + p_f E(\varepsilon_{relay}))}{x+1}dx. \tag{36}$$

This, at $\eta = 4$, can be obtained as

$$\begin{aligned} AT_s &= B(1-D_H)\int_0^\infty 1-\Bigg((1-p_f)\Big\{1-\exp\Big(\frac{-\sigma^2 x}{P_s r_s^{-4}}-\lambda_s\rho_p \\ &\times\Big(\frac{\pi^2}{2}r_s^2\sqrt{x}-\pi\frac{\tan^{-1}(\frac{d^2}{\sqrt{x}r_s^2})}{\frac{1}{\sqrt{x}r_s^2}}\Big) \\ &-\frac{\pi^2}{2}\Big(\lambda_p\sqrt{\frac{xP_p}{P_s}}r_s^2+\lambda_r\sqrt{x}r_s^2\Big)\Big)\Big\} \\ &+p_f\Big\{\Big(1-\exp\Big(\frac{-\sigma^2 x}{P_s r_s^{-4}}-\lambda_s\rho_p\Big(\frac{\pi^2}{2}r_s^2\sqrt{x}-\pi\frac{\tan^{-1}(\frac{d^2}{\sqrt{x}r_s^2})}{\frac{1}{\sqrt{x}r_s^2}}\Big) \\ &-\frac{\pi^2}{2}\Big(\lambda_p\sqrt{\frac{xP_p}{P_s}}r_s^2+\lambda_r\sqrt{x}r_R^2\Big)\Big)\Big) \\ &\times\Big\{\Big(1-\exp\Big(\frac{-\sigma^2 x}{2P_s r_{s2}^{-4}}-\lambda_s\rho_p \\ &\times\Big(\frac{\pi^2}{2\sqrt{\frac{2}{xr_s^4}}}-\pi\frac{\tan^{-1}(\sqrt{\frac{2}{xr_s^4}}d^2)}{\sqrt{\frac{2}{xr_s^4}}}\Big) \\ &-\frac{\pi^2}{2}\Big(\lambda_p\sqrt{\frac{xP_p}{2P_s}}r_s^2+\lambda_r\sqrt{\frac{x}{2}}r_R^2\Big)\Big)\Big) \\ &+\exp\Big(\frac{-\sigma^2 x}{P_s r_s^{-4}}-\lambda_s\rho_p\Big(\frac{\pi^2}{2}r_s^2\sqrt{x}-\pi\frac{\tan^{-1}(\frac{d^2}{\sqrt{x}r_s^2})}{\frac{1}{\sqrt{x}r_s^2}}\Big) \\ &-\frac{\pi^2}{2}\Big(\lambda_p\sqrt{\frac{xP_p}{P_s}}r_s^2+\lambda_r\sqrt{x}r_R^2\Big)\Big) \\ &\times\Big(1-\exp\Big(\frac{x\sigma^2}{P_s r_s^{-4}+P_r r_R^{-4}}-2\pi\lambda_s\rho_p \\ &\times\Big(\frac{\pi}{4(\sqrt{\frac{r_s^{-4}+r_R^{-4}}{x}})}-\frac{\tan^{-1}(\frac{r_s^{-4}+r_R^{-4}}{x}d^2)}{2(\frac{r_s^{-4}+r_R^{-4}}{x})}\Big) \\ &-\frac{\pi^2}{2}\Big(\lambda_r\sqrt{\frac{x}{r_s^{-4}+r_R^{-4}}}+\lambda_p\sqrt{\frac{xP_p}{P_s r_s^{-4}+P_r r_R^{-4}}}\Big)\Big)\Big)\Big\}\Bigg) \\ &\times\frac{1}{x+1}dx. \end{aligned} \tag{37}$$

V. NUMERICAL RESULTS

We now carry out the numerical simulations of the analytical approach presented in the previous sections in order to demonstrate the performance of the analyses. We carried out the Monte Carlo simulation averaged over 50 000 channel realizations in order to validate the presented analytical approach. Except when stated otherwise, the following parameters were used in the simulations: $P_p = 0$ dB, $P_s = -32$ dB, $\eta = 4$, $\sigma^2 = -180$ dB, $\lambda_s = 0.3$, $\lambda_p = 0.03$, $\theta_s = \theta_p = 3$, $r_p = 0.5$, $r_s = 0.1$, $m = 81$, $d \approx 0.295$ and the channel bandwidth was set at $B = 1$ MHz.

The effects of the SINR threshold on outage probability as presented in Fig. 2 shows that the SU outage probability is directly proportional to the SINR threshold required to guarantee coverage between any typical transmitter and its paired receiver. The relationship is the same for PUs. Interestingly, the proposed model is able to further reduce the outage probability, hence improving the user's coverage when the SINR threshold increases while other parameters remain constant. With an increase in the intensity of RNs inside the

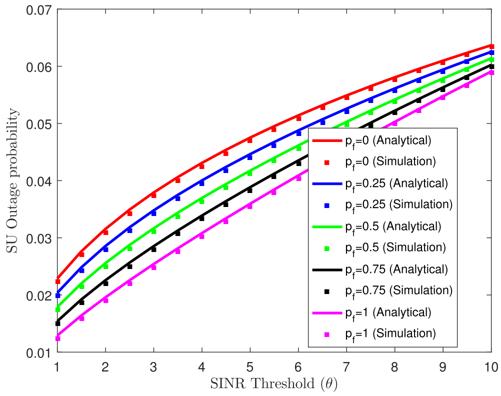

FIGURE 2. Effects of high SINR threshold on SU outage probability.

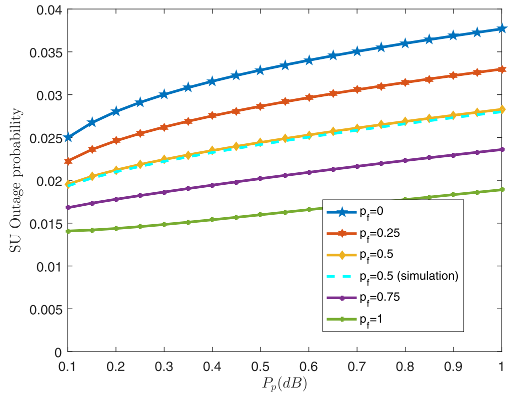

FIGURE 4. SU outage probability with increase in PU transmit power.

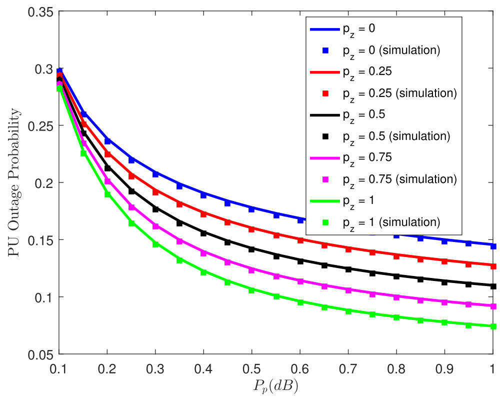

FIGURE 3. PU outage probability with increase in PU transmit power.

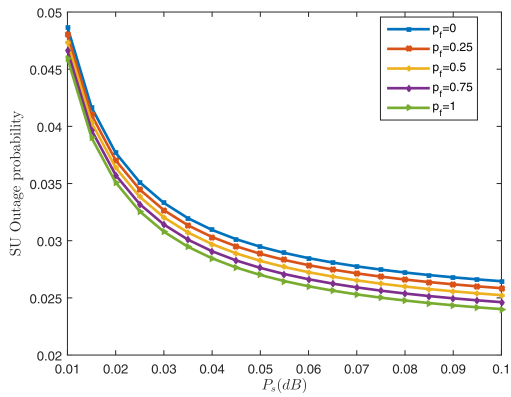

FIGURE 5. SU outage probability with increase in SU transmit power.

coverage region of the tagged receiver, the analysis showed that coverage can be improved. Depending on the user's QoS requirement, the proposed model can help a typical transmitter to meet the SINR requirement at the intended receiver especially when the intended receiver is located outside the coverage region of such typical transmitter. Although the analysis of the outage probability for each network was based on the use of stationary point process analysis, simulation results show that such analysis accurately captures the performance of mobile users.

At the constant SINR threshold, an increase in PT transmit power reduces outage in the primary network since an increase in transmit power at any typical PT is expected to improve coverage at its pair receiver provided that interference received at such a receiver remains constant. An increase in the transmit power of PT hence continues to produce a decrease in PU outage probability until a point at which such an increase has a non-significant impact on the outage owing to other channels' parameters such as interference, shadowing and fading. Improved performance was observed when $p_z = 1$, as shown in Fig. 3. The presence of RN in the coverage area of any typical PT further reduces outage in such a primary network.

The impact of PU transmit power on SU outage probability as presented in Fig. 4 also shows that SU outage probability tends to increase with an increase in PT transmit power owing to an increase in interference from active PTs received at the tagged SR, while the outage probability at the secondary network reduces with an increase in STs' transmit power, as shown in Figure 5, because of the possibility of meeting the SINR threshold required at the tagged SR when the tagged ST transmits with higher transmit power, provided that channel conditions such as fading and shadowing remain unchanged while $P_s << P_p$. Interestingly, the presented analysis shows improved performance with a higher value of p_f in the secondary network and p_z in the primary network.

Similar analyses were obtained in [13], [14] for the primary network. Since the intra-network interference within the primary network was not captured in [14], the analysis is expected to underestimate the outage probability as presented in Fig. 6. Similarly, the approximate analysis presented in [13] produces a lower outage probability compared to our analysis in Proposition 1 owing to the fact that intra-network interference in the secondary network was not captured in [13]. Likewise, the performance at the secondary network can be significantly improved with both inter-network and intra-network interference controls in the secondary network. Similar observations were made under indirect transmission as shown in Fig. 7. Generally, an increase in D further reduces the outage probability.

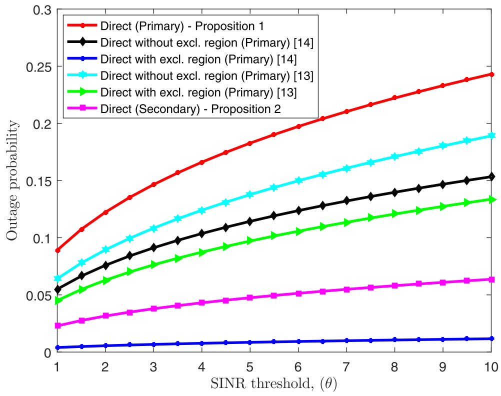

FIGURE 6. Performance of the proposed analysis under direct transmission.

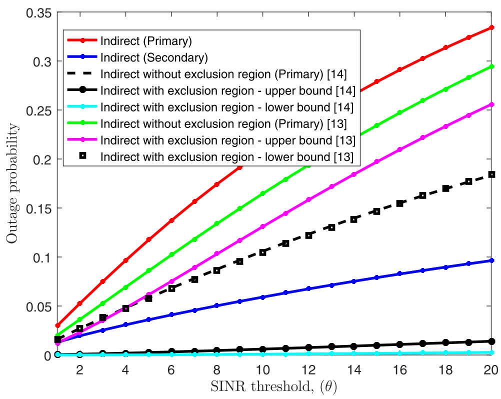

FIGURE 7. Performance of the proposed analysis under indirect transmission.

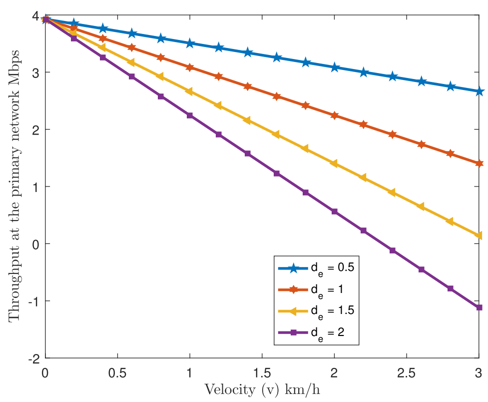

FIGURE 8. Throughput analysis at the primary network.

The effect of mobility on the performance at the primary network is presented in Fig. 8. When any tagged PR is moving at a velocity more than 2.4 km/h, the infeasible region is reached, given that the handover delay is 2 seconds. Similarly as shown in Fig. 9, the infeasible region is reached when the average velocity at any tagged SR reaches 0.7 km/h, while the handover delay is 2 seconds. This infeasible region is also reached at a velocity of 1.5 km/h when the handover delay is set at 1 second. Generally, the throughput analysis

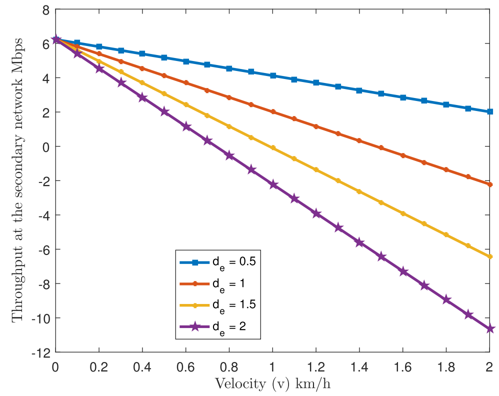

FIGURE 9. Throughput analysis at the secondary network.

presented in Fig. 8 and Fig. 9 shows improved performance when handover delay is reduced in the network, while users' throughput experience is affected by an increase in velocity. Similar results were obtained in [9], [10].

VI. CONCLUSION

Mobility in wireless communications networks remains an open issue despite its importance in realizing practical system modeling owing to the difficulty in obtaining tractable expressions for various performance metrics of interest. In this paper, we presented tractable system analyses for an orthogonal multiple access scenario by adopting multiuser diversity via packet relaying. Our analyses take into consideration various important parameters such as handover rate and spectral efficiency.

In order to avoid complicated analysis, we restricted the hop limits to two. This implies that a typical mobile receiver will experience outage if located outside the coverage area of the selected RN and its tagged transmitter, hence the mobility is restricted. In future, it will be interesting to allow unrestricted mobility in the network without compromising network performance. It will also be interesting to know whether integration of message splitting techniques will further complicate system analysis.

APPENDIX A
PROOF OF PROPOSITION 1

The outage probability at the tagged PR is given as $P(SINR_{y_k^p} \leq \theta_p)$.

$$\varepsilon_p = P\left\{\frac{P_p c_{k,k} ||y_k^p||^{-\eta}}{\sigma^2 + I_{pp} + I_{sp} + I_{rp}} \leq \theta_p\right\},$$
$$= 1 - \exp\left(\frac{-\sigma^2\theta_p}{P_p l^{-\eta}}\right)\mathcal{L}_{I_{pp}}\left(\frac{\theta_p}{P_p l^{-\eta}}\right)\mathcal{L}_{I_{sp}}\left(\frac{\theta_p}{P_p l^{-\eta}}\right)$$
$$\times \mathcal{L}_{I_{rp}}\left(\frac{\theta_p}{P_p l^{-\eta}}\right)$$

Note that the tagged mobile PR is located within the disk $b(y_k^p, D)$ centered on its pair PT, hence,

$$\varepsilon_p = 1 - \int_0^D \exp(-s\sigma^2)\mathcal{L}_{I_{pp}}(s)\mathcal{L}_{I_{sp}}(s)\mathcal{L}_{I_{rp}}(s)\frac{2l}{D^2}dl,$$

where $s = \frac{\theta_p}{P_p l^{-\eta}}$. The expression for $\mathcal{L}_{I_{pp}}$ is given as

$$\mathcal{L}_{I_{pp}}(s) = \exp\Big\{ -\pi \frac{\gamma\lambda_p (sP_p)^{\frac{\gamma}{\pi}}}{\sin(\gamma)} \Big\},$$

since PTs are distributed following PPP. Also, active ST cannot be located inside the coverage area of active PTs as well as inside the coverage area of other active STs. Hence, the expression for $\mathcal{L}_{I_{sp}}$ is given as

$$\begin{aligned}\mathcal{L}_{I_{sp}}(s) &= \exp\Big\{ -\pi \frac{\gamma\lambda_s (sP_s)^{\frac{\gamma}{\pi}}}{\sin(\gamma)} \Big\} \\ &\times \exp\Big\{ -2\pi\lambda_p \int_D^\infty \Big(1-\exp(f(v))\Big) v dv\Big\} \\ &\times \exp\Big\{ -2\pi\lambda_s^m \int_d^\infty \Big(1-\exp(f(w))\Big) w dw\Big\},\end{aligned}$$

while the distributions of RNs can be said to follow PPP with the expression for $\mathcal{L}_{I_{rp}}$ given as

$$\mathcal{L}_{I_{rp}}(s) = \exp\Big\{ -\pi \frac{\gamma\lambda_r (sP_r)^{\frac{\gamma}{\pi}}}{\sin(\gamma)} \Big\}.$$

From the given expressions for $\mathcal{L}_{I_{pp}}$, $\mathcal{L}_{I_{sp}}$ and $\mathcal{L}_{I_{rp}}$, the proof of Proposition 1 is derived.

APPENDIX B
PROOF OF PROPOSITION 2

The outage probability at the tagged SR is given as $P(SINR_{y_k^s} \leq \theta_s)$. Hence,

$$\begin{aligned}\varepsilon_s &= P\Big\{ \frac{P_s c_{k,k} ||y_k^s||^{-\eta}}{\sigma^2 + I_{ss} + I_{ps} + I_{rs}} \leq \theta_s \Big\}, \\ &= 1 - \exp\Big(\frac{-\sigma^2\theta_s}{P_s l^{-\eta}}\Big) \mathcal{L}_{I_{ss}}\Big(\frac{\theta_s}{P_s l^{-\eta}}\Big) \mathcal{L}_{I_{ps}}\Big(\frac{\theta_s}{P_s l^{-\eta}}\Big) \\ &\times \mathcal{L}_{I_{rs}}\Big(\frac{\theta_s}{P_s l^{-\eta}}\Big).\end{aligned}$$

Since the tagged SR is assumed to be distributed within the coverage region d of its paired ST,

$$\varepsilon_s = 1 - \int_0^d \exp(-z\sigma^2) \mathcal{L}_{I_{ss}}(z) \mathcal{L}_{I_{ps}}(z) \mathcal{L}_{I_{rs}}(z) \frac{2l}{d^2} dl.$$

The expression for $\mathcal{L}_{I_{ss}}$, $\mathcal{L}_{I_{ps}}$ and $\mathcal{L}_{I_{rs}}$ can be derived as

$$\mathcal{L}_{I_{ss}}(z) = \exp\Big\{ -2\pi\lambda_s\rho_p \int_d^\infty \frac{r}{1+\frac{r^\eta}{zP_s}} dr\Big\},$$

$$\begin{aligned}\mathcal{L}_{I_{ps}}(z) &= \exp\Big\{ -\pi \frac{\gamma\lambda_p (zP_p)^{\frac{\gamma}{\pi}}}{\sin(\gamma)} \Big\} \\ &\times \exp\Big\{ 2\lambda_p \int_{v-d}^{v+d} cos^{-1}\Big(\frac{-d^2+v^2+r^2}{2vr}\Big) \\ &\times \frac{r}{1+\frac{r^\eta}{zP_p}} dr\Big\},\end{aligned}$$

$$\mathcal{L}_{I_{rs}}(z) = \exp\Big\{ -\pi \frac{\gamma\lambda_r (zP_r)^{\frac{\gamma}{\pi}}}{\sin(\gamma)} \Big\}.$$

From these, the proof of Proposition 2 is derived.

REFERENCES

[1] J. G. Andrews, F. Baccelli, and R. K. Ganti, "A tractable approach to coverage and rate in cellular networks," *IEEE Trans. Commun.*, vol. 59, no. 11, pp. 3122–3134, Nov. 2011.
[2] H. ElSawy, E. Hossain, and M. Haenggi, "Stochastic geometry for modeling, analysis, and design of multi-tier and cognitive cellular wireless networks: A survey," *IEEE Commun. Surveys Tuts.*, vol. 15, no. 3, pp. 996–1019, 3rd Quart., 2013.
[3] M. Grossglauser and D. N. C. Tse, "Mobility increases the capacity of ad hoc wireless networks," *IEEE/ACM Trans. Netw.*, vol. 10, no. 4, pp. 477–486, Aug. 2002.
[4] W.-Y. Lee and I. F. Akyildiz, "Spectrum-aware mobility management in cognitive radio cellular networks," *IEEE Trans. Mobile Comput.*, vol. 11, no. 4, pp. 529–542, Apr. 2012.
[5] W. Bao and B. Liang, "Stochastic geometric analysis of user mobility in heterogeneous wireless networks," *IEEE J. Sel. Areas Commun.*, vol. 33, no. 10, pp. 2212–2225, Oct. 2015.
[6] H. Tabassum, M. Salehi, and E. Hossain, "Fundamentals of mobility-aware performance characterization of cellular networks: A tutorial," *IEEE Commun. Surveys Tuts.*, vol. 21, no.3, pp. 2288–2308, 3rd Quart., 2019.
[7] R. Arshad, H. ElSawy, S. Sorour, T. Y. Al-Naffouri, and M.-S. Alouini, "Handover management in dense cellular networks: A stochastic geometry approach," in *Proc. IEEE Int. Conf. Commun. (ICC)*, Kuala Lumpur, Malaysia, May 2016, pp. 1–7.
[8] R. Arshad, H. ElSawy, S. Sorour, T. Y. Al-Naffouri, and M.-S. Alouini, "Cooperative handover management in dense cellular networks," in *Proc. IEEE Global Commun. Conf. (GLOBECOM)*, Washington, DC, USA, Dec. 2016, pp. 1–6.
[9] R. Arshad, H. Elsawy, S. Sorour, T. Y. Al-Naffouri, and M.-S. Alouini, "Handover management in 5G and beyond: A topology aware skipping approach," *IEEE Access*, vol. 4, pp. 9073–9081, 2016.
[10] R. Arshad, H. ElSawy, S. Sorour, T. Y. Al-Naffouri, and M.-S. Alouini, "Velocity-aware handover management in two-tier cellular networks," *IEEE Trans. Wireless Commun.*, vol. 16, no. 3, pp. 1851–1867, Mar. 2017.
[11] M. N. Hindia, M. M. Fadoul, T. Abdul Rahman, and I. S. Amiri, "A stochastic geometry approach to full-duplex MIMO relay network," *Wireless Commun. Mobile Comput.*, vol. 2018, pp. 1–11, 2018. Art. no. 8342156
[12] D. Deng, M. Yu, J. Xia, Z. Na, J. Zhao, and Q. Yang, "Wireless powered cooperative communications with direct links over correlated channels," *Phys. Commun.*, vol. 28, pp. 147–153, Jun. 2018.
[13] L. Wang and V. Fodor, "On the gain of primary exclusion region and vertical cooperation in spectrum sharing wireless networks," *IEEE Trans. Veh. Technol.*, vol. 61, no. 8, pp. 3746–3758, Oct. 2012.
[14] L. Wang and V. Fodor, "On the gain of vertical cooperation in cognitive radio networks," in *Proc. IEEE Int. Conf. Commun. (ICC)*, Jun. 2011, pp. 1–6.
[15] O. Sahin, E. Erkip, and O. Simeone, "Interference channel with a relay: Models, relaying strategies, bounds," in *Proc. Inf. Theory Appl. Workshop*, San Diego, CA, USA, Feb. 2009, pp. 90–95.
[16] L. Wang and V. Fodor, "Dynamic cooperative secondary access in hierarchical spectrum sharing networks," *IEEE Trans. Wireless Commun.*, vol. 13, no. 11, pp. 6068–6080, Nov. 2014.
[17] Y. Xu, L. Wang, C. Fischione, and V. Fodor, "Distributed spectrum leasing via vertical cooperation in spectrum sharing networks," in *Proc. 9th Int. Conf. Cognit. Radio Oriented Wireless Netw.*, Oulu, Finland, 2014, pp. 185–190.
[18] X. Yue, Y. Liu, S. Kang, A. Nallanathan, and Y. Chen, "Modeling and analysis of two-way relay non-orthogonal multiple access systems," *IEEE Trans. Commun.*, vol. 66, no. 9, p. 3784—3796, Sep. 2018.
[19] P. Li, M. Rong, T. Liu, and D. Yu, "Interference modeling and analysis in two-hop cellular network with fixed relays in FDD mode," in *Proc. Int. Conf. Wireless Commun.*, vol. 1, Sep. 2005, pp. 427–451.
[20] P. Gupta and P. R. Kumar, "The capacity of wireless networks," *IEEE Trans. Inf. Theory*, vol. 46, no. 2, pp. 388–404, Mar. 2000.
[21] J. N. Laneman, D. N. Tse, and G. W. Wornell, "Cooperative diversity in wireless networks: Efficient protocols and outage behaviour," *IEEE Trans. Inf. Theory*, vol. 50, no. 12, pp. 3062–3080, Dec. 2004.
[22] M. N. Hindia, F. Qamar, T. A. Rahman, and I. S. Amiri, "A stochastic geometrical approach for full-duplex MIMO relaying model of high-density network," *Ad Hoc Netw.*, vol. 74, pp. 34–46, May 2018.

[23] Q. Zhang, J. Jia, and J. Zhang, "Cooperative relay to improve diversity in cognitive radio networks," *IEEE Commun. Mag.*, vol. 47, no. 2, pp. 111–117, Feb. 2009.

[24] B. Zhong and Z. Zhang, "Opportunistic two-way full-duplex relay selection in underlay cognitive networks," *IEEE Syst. J.*, vol. 12, no. 1, pp. 725–734, Mar. 2018.

[25] S. D. Okegbile, B. T. Maharaj, and A. S. Alfa, "Relaying techniques based outage analysis for mobile users in cognitive radio networks," in *Proc. IEEE 91st Veh. Technol. Conf. (VTC-Spring)*, Antwerp, Belgium, May 2020, pp. 1–5.

[26] M. Stemm and R. H. Katz, "Vertical handoffs in wireless overlay networks," *Mobile Netw. Appl.*, vol. 3, no. 4, pp. 335–350, Jan. 1998.

[27] J. McNair and F. Zhu, "Vertical handoffs in fourth-generation multinetwork environments," *IEEE Wireless Commun.*, vol. 11, no. 3, pp. 8–15, Jun. 2004.

[28] S. D. Okegbile, B. T. Maharaj, and A. S. Alfa, "Spatiotemporal characterization of Users' experience in massive cognitive radio networks," *IEEE Access*, vol. 8, pp. 57114–57125, 2020.

[29] S. D. Okegbile, B. T. Maharaj, and A. S. Alfa, "Interference characterization in underlay cognitive networks with intra-network and inter-network dependence," *IEEE Trans. Mobile Comput.*, early access, May 8, 2020, doi: 10.1109/TMC.2020.2993408.

[30] P. Cardieri, "Modeling interference in wireless ad hoc networks," *IEEE Commun. Surveys Tuts.*, vol. 12, no. 4, pp. 551–572, 1st Quart., 2010.

[31] C. Bettstetter, G. Resta, and P. Santi, "The node distribution of the random waypoint mobility model for wireless ad hoc networks," *IEEE Trans. Mobile Comput.*, vol. 2, no. 3, pp. 257–269, Jul. 2003.

[32] Z. Gong and M. Haenggi, "Interference and outage in mobile random networks: Expectation, distribution, and correlation," *IEEE Trans. Mobile Comput.*, vol. 13, no. 2, pp. 337–349, Feb. 2014.

[33] A. Wittneben, I. Hammerstrom, and M. Kuhn, "Joint cooperative diversity and scheduling in low mobility wireless networks," in *Proc. IEEE Global Telecommun. Conf.*, Nov. 2004, pp. 780–784.

[34] D. Hong and S. S. Rappaport, "Traffic model and performance analysis for cellular mobile radio telephone systems with prioritized and nonprioritized handoff procedures," *IEEE Trans. Veh. Technol.*, vol. 35, no. 3, pp. 77–92, Aug. 1986.

[35] M. M. Zonoozi and P. Dassanayake, "User mobility modeling and characterization of mobility patterns," *IEEE J. Sel. Areas Commun.*, vol. 15, no. 7, pp. 1239–1252, Sep. 1997.

[36] K. L. Yeung and S. Nanda, "Optimal mobile-determined micro-macro cell selection," in *Proc. IEEE Int. Symp. Personal, Indoor Mobile Radio Commun.*, Toronto, ON, Canada, vol. 1, Sep. 1995, pp. 294–299.

[37] B. Figliuzzi, "Introduction to stochastic geometry," Tech. Rep., 2015. [Online]. Available: http://www.cmm.mines-paristech.fr/~figliuzzi/Stochastic_Geometry.pdf

[38] C.-H. Lee and M. Haenggi, "Interference and outage in Poisson cognitive networks," *IEEE Trans. Wireless Commun.*, vol. 11, no. 4, pp. 1392–1401, Apr. 2012.

[39] X. Lin, R. K. Ganti, P. J. Fleming, and J. G. Andrews, "Towards understanding the fundamentals of mobility in cellular networks," *IEEE Trans. Wireless Commun.*, vol. 12, no. 4, pp. 1686–1698, Apr. 2013.

SAMUEL D. OKEGBILE (Graduate Student Member, IEEE) received the B.Tech. (Hons.) degree in computer engineering (First class division) from the Ladoke Akintola University of Technology, Ogbomoso, Nigeria, in 2011, and the M.Sc. degree in computer science (Distinction) from Obafemi Awolowo University, Ile-Ife, Nigeria, in 2016. He is currently pursuing the Ph.D. degree in computer engineering with the Department of Electrical, Electronic and Computer Engineering, University of Pretoria, South Africa. His research interests are in the area of pervasive and mobile computing, which includes various interesting topics on cognitive radio networks, the Internet of Things, and wireless sensor networks.

BODHASWAR T. MAHARAJ (Senior Member, IEEE) received the Ph.D. degree in wireless communications from the University of Pretoria, South Africa. He is currently a Professor and holds the position of Sentech Chair of Broadband Wireless Multimedia Communications with the Department of Electrical, Electronic, and Computer Engineering, University of Pretoria. His research interests are in MIMO channel modeling, OFDM-MIMO systems, and cognitive radio for rural broadband.

ATTAHIRU S. ALFA (Member, IEEE) is currently a Professor Emeritus at the Department of Electrical and Computer Engineering, University of Manitoba, and an Extraordinary Professor at the Department of Electrical, Electronic and Computer Engineering, University of Pretoria. Some of his previous works include developing efficient decoding algorithms for LDPC codes, channel modeling, traffic estimation for the Internet, and cross-layer analysis. He also works in the application of queuing theory to other areas such as transportation systems, manufacturing systems, and healthcare systems. He has authored two books: "*Queueing Theory for Telecommunications: Discrete Time Modelling of a Single Node System*" (Springer, 2010); "*Applied Discrete-Time Queue*" (Springer, 2015) second edition of the first book; and has also coauthored (with Dr. Ibrahim) a book: "*Optimization Methods for User Admissions and Radio Resource Allocation for Multicasting over High Altitude Platforms*" (River Publishers, 2019). His most recent research focus covers the age of information, wireless sensor networks, cognitive radio networks, network restoration tools for wireless sensor networks, and the role of 5G in the IoT, with a specific interest in the mathematical modeling of those systems. His general research covers, among others, the following areas: queuing theory and applications, optimization, performance analysis and resource allocation in telecommunication systems, modeling of communication networks, analysis of cognitive radio networks, modeling and analysis of wireless sensor networks, and smart cities.